Impact of a conformationally restricted receptor on the BF_2 chelated azadipyrromethene fluorosensing platform†

John Killoran and Donal F. O'Shea*

Received (in Cambridge, UK) 30th September 2005, Accepted 27th January 2006
First published as an Advance Article on the web 27th February 2006
DOI: 10.1039/b513878g

Conformational control of the receptor–fluorophore orientation of BF_2 chelated azadipyrromethene sensors reveals two photophysically different modes of analyte triggered fluorescence switching both of which exhibit large off–on fluorescence intensity responses to the light input–output of the sensors in the visible red spectral region.

The development of new molecular fluorescent sensor platforms for *in vivo* and *in vitro* analysis has emerged as an actively investigated research field in recent years. In particular, fluorophores which absorb and emit in the visible red and near-infrared (NIR) spectral regions are much sought after for application in areas such as tumour imaging, drug discovery and assay development.[1] The use of this spectral region is ideally suited to these applications due to minimal endogenous chromophore absorption and autofluorescence. Examples of chromophore classes which have been used to address this spectral region are the cyanines,[2] squaraines,[3] modified BODIPY dyes[4] and *N*-phenyl-1,8,-naphthalimides.[5] The BF_2 chelated tetraarylazadipyrromethenes **1** have been recently reported as a new class of chromophore with high absorption extinction coefficients (70–80 000 M^{-1} cm^{-1}) and fluorescence quantum yields (0.23–0.36) between 650 and 750 nm (Fig. 1).[6] We are currently advancing the application of this class to visible red and NIR molecular fluorescent sensors.

The design of fluorescent probes typically adopts a modular receptor–spacer–fluorophore approach. The function of the receptor is to detect the targeted analyte, whereas the role of the fluorophore is to quantify and relay this detection. The purpose of the spacer unit is to join the fluorophore to the receptor whilst keeping the ground state electronic systems of the receptor and the fluorophore disconnected. The most commonly used spacer is a saturated methylene unit (C_1 spacer), which effectively decouples

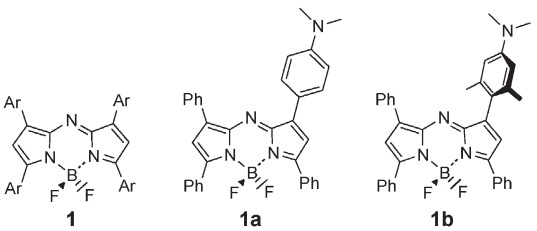

Fig. 1 BF_2 chelated tetraarylazadipyrromethenes.

Centre for Synthesis and Chemical Biology, Conway Institute, School of Chemistry and Chemical Biology, University College Dublin, Belfield, Dublin 4, Ireland. E-mail: donal.f.oshea@ucd.ie; Tel: +353(0)17162425
† Electronic supplementary information (ESI) available: Experimental procedures and analytical data, for **1a** and **1b**. Photophysical organic solvent study of **1b**. X-Ray crystallographic data of **1a** and **1b**. See DOI: 10.1039/b513878g

the system.[7] The electronic separation of receptor and fluorophore can also be accomplished by a virtual spacer (C_0), though this approach is significantly less exploited (Fig. 2A).[8] In this approach, the receptor is covalently linked directly to the fluorophore but their electronic systems remain disconnected as a result of a forced orthogonal conformation between the receptor and fluorophore. If a near orthogonal conformation exists, the electron system of the receptor remains decoupled from that of the fluorophore due to restricted π-orbital overlap. If this pre-orientation does not exist then an integrated, or intrinsic, receptor–fluorophore is generated in which there is no electronic separation of receptor and fluorophore (Fig. 2B). In this case switching is modulated by an internal charge transfer (ICT) process with integrated sensors often having responses both in the ground state and the excited state during substrate recognition.[9]

To determine the sensing potential and impact of non-restricted and restricted aniline receptors, we chose to synthesize and examine the photophysical properties of **1a** and **1b** (Fig. 1). We anticipated that both would have the potential to be off–on pH responsive sensors and, as anilino nitrogens (as part of a more structurally elaborate receptor) often control the recognition response to metal ions such as Ca^{2+} and Mg^{2+}, we anticipated that examination of **1a** and **1b** would delineate the design criteria for future receptors.[10]

We have employed a modular building block approach to the synthesis of our target compounds by the condensation of 2,4-diaryl-5-nitroso-pyrroles with 2,4-diarylpyrroles (Scheme 1).[11] We have previously described efficient routes to 2,4-diarylpyrroles and their α-nitroso derivatives.[11,12] The generation of the tetraarylazadipyrromethene **4a** was achieved by the condensation of 2-nitroso-3,5-diphenylpyrrole **3a** with the receptor functionalised 2,4-diarylpyrrole **2a**. Tetraarylazadipyrromethene **4b** was formed from the reaction of 2,4-diphenylpyrrole **2b** with the 2-nitroso-3,5-diarylpyrrole **3b**. The final BF_2-chelation step to yield sensors **1a** and **1b** was achieved by the room temperature reaction of **3a** or **3b** with borontrifluoride diethyletherate with base in dichloromethane.

In order to obtain aqueous solutions of **1a,b** for spectroscopic analysis the emulsifier Cremophor EL (CrEL) was used. CrEL is

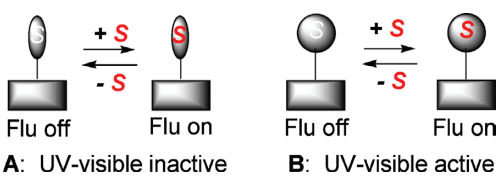

Fig. 2 A; Schematic of a fluorescent sensor with a virtual spacer. Rectangle = fluorophore; oval = orthogonal receptor for substrate **S**; **S** = substrate. B; Schematic of an intergral fluorescent sensor. Rectangle = fluorophore; circle = co-planar receptor for substrate **S**; **S** = substrate.

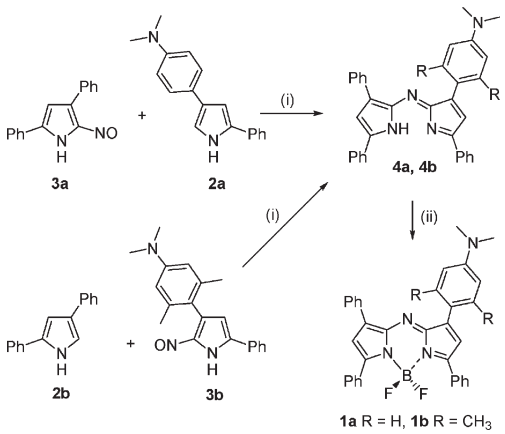

Scheme 1 Synthetic routes to **1a** and **1b**. (i) Acetic anhydride, acetic acid, 100 °C, 1 h. (ii) $BF_3{\cdot}OEt_2$, DIEA, CH_2Cl_2, rt, 6 h.

frequently exploited *in vivo* as a delivery agent for drugs with poor water solubility and we have found it suitable for the cellular delivery of a range of analogues of **1**.[6b]

We first examined the excited state response of aqueous formulated solutions of **1a** to varying acidic conditions. We were pleased to observe virtually complete quenching of the fluorescence in the pH range where the amine receptor remained unprotonated (Fig. 3, green trace). Upon protonation, the fluorescence spectrum showed a strong proton induced fluorescence enhancement with a wavelength of maximum fluorescence at 683 nm (Fig. 3, red trace). A sigmoidal plot of pH *versus* fluorescence intensity predicted an apparent pK_a of less than 1.0 (Fig. 3, inset).[13] Encouragingly, the enhancement of fluorescence intensity was greater than 250 fold between the sensor off and on positions. We anticipated the lack of a disconnecting modality between the receptor and fluorophore in **1a** would facilitate an ICT between the receptor and the fluorophore sub-units resulting in quenching of fluorescence at higher pH values, but that upon protonation the ICT would be suppressed and a strong fluorescence established.

A consequence of exploiting ICT formation as an excited state quenching mechanism is the reorganisation of the ground state properties of **1a** upon analyte recognition. The absorbance spectrum of unprotonated **1a** has two bands in the red spectral region centred at 618 and 750 nm (Fig. 4, green trace). At pH values less than 2, upon protonation of the receptor, the absorbance bands at 618 and 750 nm progressively reduced in intensity and a new

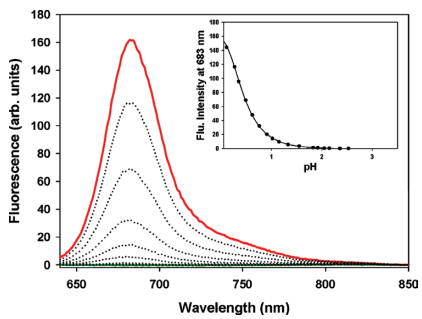

Fig. 3 pH responsive fluorescence spectra of **1a**. Red trace pH = ~0.2, green trace pH = 2.5. Excitation at 630 nm, slit widths 5 nm, 1×10^{-6} M in water–CrEL. I_{NaCl} = 150 mmol L^{-1}. Inset shows the sigmoidal plot predicting an apparent pK_a value less than 1.0 at 25 °C.

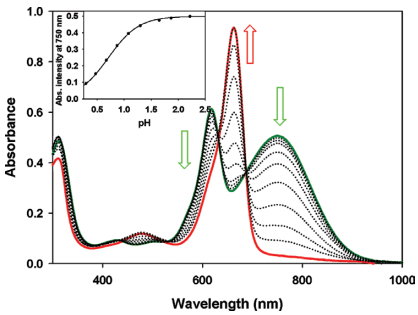

Fig. 4 pH responsive absorbance spectra using a 1×10^{-5} M solution of **1a** in water–CrEL. Red trace pH = ~0.2, green trace pH = 2.5. I_{NaCl} = 150 mmol L^{-1}. Inset shows the sigmoidal plot predicting an apparent pK_a value of less than 1.0 at 25 °C.

single band appeared at 662 nm (Fig. 4, red trace). Plotting the disappearance of the 750 nm band against pH gave a similar sigmoidal response to the fluorescence titration (Fig. 4, inset).

The UV-visible spectral characteristics are indicative of a co-planar receptor–fluorophore orientation in **1a**. The molecular structure of **1a**, obtained by X-ray crystallography, confirmed a small torsion angle about the receptor–fluorophore bond of only 18.5° (Fig. 5).‡

We expected that the introduction of methyl groups on the anilino ring of **1b** would exert a steric influence on the conformation about the aryl–fluorophore bond. Excitation of **1b** at 630 nm in aqueous media gave a very weak emission when unprotonated but showed a strong acid induced fluorescence enhancement with a λ maximum at 673 nm and a fluorescence intensity enhancement in excess of 250 fold (Fig. 6). A plot of pH *versus* fluorescence provided a sigmoidal curve, which calculated an apparent pK_a of 2.0 (Fig. 6, inset). This higher value when compared to **1a** would indicate that some disconnection of the sensor sub-units had been achieved.

This was corroborated by examination of the absorbance properties during analyte detection. The visible red absorbance spectrum of unprotonated **1b** revealed that it consisted of a single band with a wavelength maximum of 639 nm (Fig. 7, green trace). During acid titration minor changes were recorded with the λ maximum undergoing a small bathochromic shift to 651 nm and the bandwidth decreasing. Overall the variations were minor especially when compared to **1a** and provide a powerful demonstration of the effects of sub-unit pre-orientation in fluorescence sensor design. A single crystal X-ray structure revealed that the torsion angle between the receptor and fluorophore had increased to 53.4(7)° as a result of the methyl substituents (Fig. 8).§

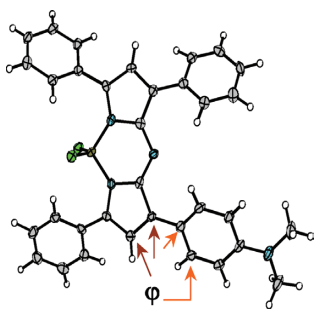

Fig. 5 X-Ray crystal structure of **1a**. Torsion angle (φ) C24–C25–C27–C28 (marked by arrows) = 18.5(9)°.

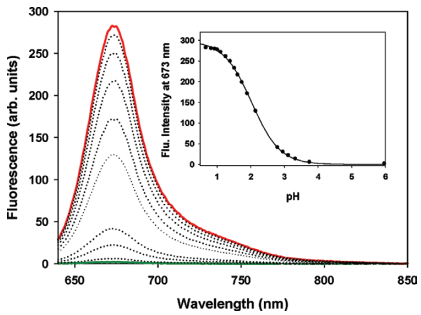

Fig. 6 pH responsive fluorescence spectra of **1b**. Red trace pH = 1.0, green trace pH = 4.0. Excitation at 630 nm, slit widths 5 nm, 1×10^{-6} M in water–CrEL. I_{NaCl} = 150 mmol L^{-1}. Insert shows the sigmoidal plot predicting an apparent pK_a value of 2.0 at 25 °C.

As the effect of microenvironment polarity on excited state sensing mechanisms is well established,[14] we have examined the emission sensitivity of **1a,b** to polarity changes by determining the spectral properties in four solvents of varying dipolarity. We were pleased to observe that emissions from unprotonated **1a,b** in DMF, THF, 1,4-dioxane and cyclohexane were very weak and in each case large fluorescence enhancements were recorded upon addition of trifluoroacetic acid (ESI†).

In conclusion, we have outlined the flexible modular synthesis of a new class of visible red fluorosensors based upon either an integrated or virtual spacer design. Sensor performance is excellent with large off–on fluorescence intensity responses and low microenvironment polarity effects. The ability to control the analyte induced photophysical responses by subtle conformational changes would allow for the tailoring of sensor properties to an application requirement. In addition the described synthetic route would readily allow for analogues functionalised with other substrate specific receptors to be generated.

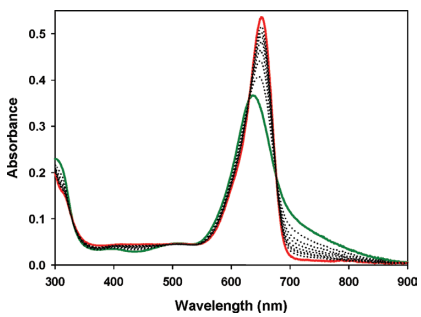

Fig. 7 pH responsive absorbance spectra using a 1×10^{-5} M solution of **1b** in water–CrEL. Red trace pH = 1.0, green trace pH = 4.0. I_{NaCl} = 150 mmol L^{-1}.

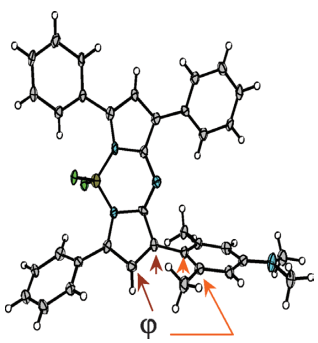

Fig. 8 X-Ray crystal structure of **1b**. Torsion angle (φ) C19–C18–C21–C26 (marked by arrows) = 53.4(7)°.

This work was supported by the Program for Research in Third-Level Institutions administered by the HEA. We thank Dr D. Rai of the CSCB Mass Spectrometry Centre and Dr H. Mueller-Bunz of the UCD Crystallographic Centre for analyses.

Notes and references

‡ Crystal data for compound **1a**: $C_{34}H_{27}BN_4F_2$, M = 540.41, triclinic, $P\bar{1}$ (#2), a = 10.755(3), b = 10.824(3), c = 12.163(4) Å, V = 1288.9(7) Å^3, μ(Mo-Kα) = 0.710 mm^{-1}, T = 113(2) K, Z = 2, D_c = 1.392 Mg m^{-3}, F(000) = 564, independent reflections 4977 (R_{int} = 0.0530). Final R for reflections with $I > 2\sigma(I)$ R_1 = 0.0944, wR_2 = 0.2168, for all data R_1 = 0.1443, wR_2 = 0.2358. CCDC 285002.

§ Crystal data for compound **1b**: $C_{36}H_{31}BN_4F_2$, M = 68.46, monoclinic, $C2$, a = 42.555(7), b = 5.3195(9), c = 12.781(2) Å, V = 2814.3(8) Å^3, μ(Mo-Kα) = 0.710 mm^{-1}, T = 293(2) K, Z = 4, D_c = 1.342 Mg m^{-3}, F(000) = 1192, independent reflections 3777 (R_{int} = 0.0602). Final R for reflections with $I > 2\sigma(I)$ R_1 = 0.0509, wR_2 = 0.0981, for all data R_1 = 0.0854, wR_2 = 0.1109. CCDC 285001. For crystallographic data in CIF or other electronic format see DOI: 10.1039/b513878g

1 (*a*) V. Ntziachristos, J. Ripoll, L. V. Wang and R. Weissleder, *Nat. Biotechnol.*, 2005, **23**, 313; (*b*) R. Weissleder, *Nat. Rev.*, 2002, **2**, 1; (*c*) M. Rudin and R. Weissleder, *Nat. Rev.*, 2003, **2**, 123; P. Mitchell, *Nat. Biotechnol.*, 2001, **19**, 1013.

2 (*a*) X. Peng, F. Song, B. Lu, Y. Wang, W. Zhou, J. Fan and Y. Gao, *J. Am. Chem. Soc.*, 2005, **127**, 4170; (*b*) B. Ozmen and B. U. Akkaya, *Tetrahedron Lett.*, 2000, **41**, 9185.

3 (*a*) B. Arunkumar and A. Ajayaghosh, *Chem. Commun.*, 2005, 599; (*b*) W. Pham, R. Weissleder and C.-H. Tung, *Angew. Chem., Int. Ed.*, 2002, **41**, 3659; (*c*) U. Oguz and B. U. Akkaya, *J. Org. Chem.*, 1998, **63**, 6059.

4 (*a*) Z. Shen, H. Röhr, K. Rurack, H. Uno, M. Spieles, B. Schulz, G. Reck and N. Ono, *Chem.–Eur. J.*, 2004, **10**, 4853; (*b*) K. Rurack, M. Kollmannsberger and J. Daub, *Angew. Chem., Int. Ed.*, 2001, **40**, 385.

5 K. Rurack, U. Resch-Genger, J. L. Bricks and M. Spieles, *Chem. Commun.*, 2000, 2103.

6 (*a*) J. Killoran, L. Allen, J. F. Gallagher, W. M. Gallagher and D. F. O'Shea, *Chem. Commun.*, 2002, 1862; (*b*) A. Gorman, J. Killoran, C. O'Shea, T. Kenna, W. M. Gallagher and D. F. O'Shea, *J. Am. Chem. Soc.*, 2004, **126**, 10619; (*c*) W. M. Gallagher, L. T. Allen, C. O'Shea, T. Kenna, M. Hall, J. Killoran and D. F. O'Shea, *Br. J. Cancer*, 2005, **92**, 1702; (*d*) S. O. McDonnell, M. J. Hall, L. T. Allen, A. Byrne, W. M. Gallagher and D. F. O'Shea, *J. Am. Chem. Soc.*, 2005, **127**, 16360.

7 A. P. de Silva, H. Q. N. Gunaratne, T. Gunnlaugsson, A. J. M. Huxley, C. P. McCoy, J. T. Rademacher and T. B. Rice, *Chem. Rev.*, 1997, **97**, 1515.

8 (*a*) K. Rurack and U. Resch-Genger, *Chem. Soc. Rev.*, 2002, **31**, 116; (*b*) M. Maus and K. Rurack, *New J. Chem.*, 2000, **24**, 677; (*c*) M. Kollmannsberger, T. Gareis, S. Heinl, J. Breu and J. Daub, *Angew. Chem., Int. Ed. Engl.*, 1997, **36**, 1333.

9 (*a*) J. F. Callan, A. P. de Silva, J. Ferguson, A. J. M. Huxley and A. M. O'Brien, *Tetrahedron*, 2004, **60**, 11125; (*b*) K. Rurack, A. Danel, K. Rotkiewicz, D. Grabka, M. Spieles and W. Rettig, *Org. Lett.*, 2002, **4**, 4647.

10 J. H. Hartley, T. D. James and C. J. Ward, *J. Chem. Soc., Perkin Trans. 1*, 2000, 3155.

11 M. J. Hall, S. O. McDonnell, J. Killoran and D. F. O'Shea, *J. Org. Chem.*, 2005, **70**, 5571.

12 J. Killoran, J. F. Gallagher, P. V. Murphy and D. F. O'Shea, *New J. Chem.*, 2005, **29**, 1258.

13 pK_a values in a micellar microenvironment are often lower than might be anticipated. M. S. Fernandez and P. Fromherz, *J. Phys. Chem.*, 1977, **81**, 1755.

14 (*a*) B. Bag and P. K. Bharadwaj, *J. Phys. Chem. B*, 2005, **109**, 4377; (*b*) R. A. Bissell, A. P. de Silva, W. T. M. L. Fernando, S. T. Patumathavithana and T. K. S. D. Samarasinghe, *Tetrahedron Lett.*, 1991, **32**, 425.